Suppression of Synaptotagmin II restrains phorbol-ester-induced downregulation of protein kinase Cα by diverting the kinase from a degradative pathway to the recycling endocytic compartment

Ze Peng, Elena Grimberg and Ronit Sagi-Eisenberg*

Department of Cell Biology and Histology, Sackler School of Medicine, Tel Aviv University, Tel Aviv, 69978, Israel
*Author for correspondence (e-mail: histol3@post.tau.ac.il)

Accepted 1 May 2002
Journal of Cell Science 115, 3083-3092 (2002) © The Company of Biologists Ltd

Summary

Downregulation of protein kinase Cα (PKCα) following long-term exposure to phorbol esters such as TPA is traffic dependent and involves delivery of the active, membrane-associated PKCα to endosomes. In this study, we show that synaptotagmin II (Syt II), a member of the Syt family of proteins, is required for TPA-induced degradation of PKCα. Thus, whereas the kinase half-life in TPA-treated cultured mast cells (the mast cell line rat basophilic leukemia RBL-2H3) is 2 hours, it is doubled in RBL-Syt II$^-$ cells, in which the cellular level of Syt II is reduced by >95% by transfection with Syt II antisense cDNA. We demonstrate that in TPA-treated RBL cells, PKCα travels from the cytosol to the plasma membrane, where it is delivered to early endosomes on its route to degradation. By contrast, in TPA-treated RBL-Syt II$^-$ cells, PKCα is diverted to recycling endosomes and remains distributed between the plasma membrane and the perinuclear recycling endocytic compartment. Notably, in both RBL and RBL-Syt II$^-$ cells, a fraction of PKCα is delivered and maintained in the secretory granules (SG). These results implicate Syt II as a critical factor for the delivery of internalized cargo for degradation. As shown here, one consequence of Syt II suppression is a delay in PKCα downregulation, resulting in its prolonged signaling.

Key words: Protein kinase C, Synaptotagmin, TPA, Mast cells, Endosome

Introduction

Protein kinase C (PKC) is a family of Ser/Thr kinases that plays a pivotal role in mediating cellular response cascades, including ones for growth and differentiation (Mellor and Parker, 1998). PKC isoforms include the Ca^{2+}- and phosphatidylserine (PS)-dependent conventional/classic PKCs, PKCα, PKCβ1, PKCβ2 and PKCγ, which require diacylglycerol (DAG) for activity, the novel Ca^{2+}-independent PKCs, PKCδ, PKCε, PKCη, PKCμ and PKCθ, which require PS and DAG for activity, and the atypical PKCs, PKCζ , PKCτ and PKCλ, which require only PS (Mellor and Parker, 1998).

Conventional and novel PKCs serve as cellular targets for tumor-promoting phorbol esters, such as 12-O-tetradecanoylphorbol-13-acetate (TPA), which induce tumors in initiated cells (Nishizuka, 1986). Acute exposure to TPA induces the translocation and activation of cytosolic TPA-responsive PKCs to the plasma membrane, whereas prolonged incubation results in the proteolytic degradation of the responsive PKCs and their depletion from the cell (Nishizuka, 1986; Mellor and Parker, 1998). Both activation and downregulation of PKCs have appreciable impacts on cellular processes and have been implicated in carcinogenesis (Nishizuka, 1986; Mellor and Parker, 1998).

Recent evidence indicates that degradation of PKCα following long-term exposure to TPA is traffic dependent and involves transport of the activated kinase from the plasma membrane to caveolae and then to an endosomal compartment (Mineo et al., 1998; Prevostel et al., 2000). Intracellular trafficking normally involves packaging of cargo into transport vesicles, which subsequently fuse with their appropriate target membranes. These processes are highly regulated, accommodating multiple regulatory proteins, including the SNAREs, which are believed to constitute the fusion machinery (Bennet, 1995; Lowe, 2000; McNew et al., 2000), and the Rab GTPases (Armstrong, 2000). Another family of proteins implicated in the control of protein traffic is the synaptotagmin (Syt) family, which comprises thirteen evolutionarily conserved and structurally related proteins (Sudhof and Rizo, 1996; Adolfsen and Littleton, 2001). Members of the Syt family display wide, yet distinct, tissue distribution, suggesting that these proteins may regulate discrete transport processes. Syt I and Syt II, the most characterized Syt homologues, have been implicated as Ca^{2+} sensors in the control of neurotransmission (Brose et al., 1992; Geppert et al., 1994). However, the role of these homologues in non-neural tissues or the role of other members of this family remains obscure.

We have previously shown that rat basophilic leukemia cells (RBL-2H3), a mucosal mast cell line, endogenously express the Syt homologues Syt II, III and V (Baram et al., 1999; Baram et al., 2001). We have further demonstrated that Syt II

is located in the RBL-2H3 cells at a late endosomal/lysosomal compartment, where it functions to negatively regulate Ca^{2+}-triggered lysosomal exocytosis (Baram et al., 1999). Because RBL cells also express PKCα (Chang et al., 1997; Razin et al., 1999), we sought to employ the RBL cells to investigate whether Syt II regulates the trafficking route leading to PKCα downregulation. Here we show that in cells in which the level of Syt II expression is reduced by >95% by antisense cDNA, the rate of TPA-induced PKCα degradation is significantly reduced. We further show that this attenuation of PKCα downregulation results from the diversion of PKCα from a degradative route towards the perinuclear recycling endocytic compartment. Our results therefore identify Syt II as a novel and critical factor required for the delivery of cargo from early endosomes to the degradative compartment as well as a novel regulator of PKCα downregulation.

Materials and Methods

Antibodies

Antibodies used included a polyclonal antibody for PKCα (Santa Cruz), a monoclonal antibody for serotonin (DAKO, Denmark), a monoclonal antibody (8G2B) directed against the N-terminal region of Syt II and a rabbit polyclonal serum against the cytoplasmic domain of Syt III (a generous gift from M. Takahashi and Y. Shoji-Kasai, Mitsubishi-Kasei Institute of Life Sciences, Tokyo, Japan), rabbit polyclonal antibodies directed against Rab11 (a generous gift from M. Zerial, EMBL), a monoclonal antibody directed against actin (Chemicon International, CA), horseradish-peroxidase (HRP)-conjugated goat anti-rabbit or anti-mouse IgG and Rhodamine- or FITC-conjugated donkey anti-rabbit or anti-mouse IgG (Jackson Research Laboratories, West Grove PA).

Cell culture

Rat basophilic leukemia cells (RBL-2H3, hereafter termed RBL cells) were maintained in adherent cultures in DMEM supplemented with 10% FCS in a humidified atmosphere of 5% CO_2 at 37°C.

Cell transfection

Syt II transfectants were generated as described previously (Baram et al., 1999). Briefly, full-length rat Syt II cDNA (generously provided by T. C. Sudhof, Howard Hughes Medical Institute, University of Texas Southwestern Medical School, Dallas, TX) was subcloned into the *Eco*RI site of the pcDNA3 expression vector (Invitrogen, San Diego, CA) both in the sense and antisense orientations. RBL cells (8×10^6) were transfected with 20 μg DNA (recombinant or empty vector) by electroporation (0.25 V, 960 μF) and immediately plated in tissue culture dishes containing growth medium (supplemented DMEM). G418 (1 mg/ml) was added 24 hours after transfection, and stable transfectants were selected within 14 days. The same procedure was employed to generate stable Syt III transfectants, except that the cells were transfected with a full-length rat Syt III cDNA (a generous gift from S. Seino, Chiba University, School of Medicine, Japan) subcloned in an anti-sense orientation into the *Hin*dIII/*Xba*I sites of the pcDNA3 expression vector.

Preparation of cell lysates

RBL cells (1×10^6) were washed in PBS and resuspended in 40 μl of lysis buffer [50 mM Hepes, pH 7.4, 150 mM NaCl, 10 mM EDTA, 2 mM EGTA, 1% Triton-X 100, 0.1% SDS, 50 mM NaF, 10 mM NaPPi, 2 mM Na_3VO_4, 1 mM PMSF, 10 μg/ml cocktail protease inhibitors (Boehringer Mannheim, Germany)]. Cell lysates were left on ice for 10 minutes and then centrifuged at 12,000 ***g*** for 15 minutes at 4°C. The cleared supernatants were mixed with 5×Laemmli sample buffer to a final concentration of 1×, boiled for 10 minutes and subjected to SDS-PAGE and immunoblotting.

Isolation of cytosolic and membranal fraction

RBL cells (1×10^6) were washed twice with cold PBS. The cytosolic fractions were extracted following 5 minutes of incubation on ice with 200 μl of buffer (0.5 mg/ml digitonin, 20 mM Mops, pH 7.2, 10 mM EGTA, 5 mM EDTA), and the membranal fractions were collected following a further 7 minutes of incubation with 200 μl of the same buffer supplemented with 0.5% Triton-X 100 (Pelech et al., 1986).

Subcellular fractionation

Cells were fractionated as previously described (Baram et al., 1999). Briefly, RBL cells (8×10^7) were washed with PBS and suspended in homogenization buffer [0.25 M sucrose, 2 mM $MgCl_2$, 800 U/ml DNase I (Sigma-Aldrich), 10 mM Hepes, pH 7.4, 1 mM PMSF and a cocktail of protease inhibitors (Boehringer Mannheim, Germany)]. Cells were subsequently disrupted by three cycles of freezing and thawing followed by 20 passages through a 21-gauge needle and 10 passages through a 25-gauge needle. Unbroken cells and nuclei were removed by centrifugation for 10 minutes at 500 ***g***, and the supernatant was sequentially filtered through 5 and 2 μm filters (Poretics Co.). The final filtrate was then loaded onto a continuous, 0.45-2.0 M sucrose gradient (10 ml), which was layered over a 0.3 ml cushion of 70% (wt/wt) sucrose and centrifuged for 18 hours at 100,000 ***g***.

SDS-PAGE and immunoblotting

Samples (normalized according to protein content or number of cells) were separated by SDS-PAGE using 7.5 or 10% polyacrylamide gels. They were then electrophoretically transferred to nitrocellulose filters. Blots were blocked for 2 hours in TBST (10 mM Tris-HCl, pH 8.0, 150 mM NaCl and 0.05% Tween 20) containing 5% skimmed milk followed by overnight incubation at 4°C with the indicated primary antibody. Blots were washed three times and incubated for 1 hour at room temperature with the secondary antibody (horseradish-peroxidase-conjugated goat anti-rabbit or anti-mouse IgG; Jackson Research Laboratories, West Grove PA). Immunoreactive bands were visualized by the enhanced chemiluminescence method (ECL) according to standard procedures.

Secretion from RBL cells

RBL cells were seeded in 24-well plates at 1×10^6 cells per well and incubated overnight in a humidified incubator at 37°C. The cells were then washed three times with Tyrode's buffer (20 mM Hepes, pH 7.4, 137 mM NaCl, 2.7 mM KCl, 0.4 mM NaH_2PO_4, 1.5 mM $CaCl_2$, 1 mM $MgCl_2$, 5 mM glucose, and 0.1% BSA) and stimulated in the same buffer with the indicated concentrations of the calcium ionophore A23187 and the phorbol ester 12-O-tetradecanoylphorbol-13-acetate (TPA; Calbiochem). Secretion was allowed to proceed for 30 minutes at 37°C. Aliquots from the supernatants were taken for measurements of released β-hexosaminidase activity as described previously (Baram et al., 1999).

Immunofluoresence and confocal analysis

Treated or untreated RBL cells (1×10^5) were grown on 12 mm round glass coverslips. For immunofluorescence experiments, cells were washed twice with PBS and fixed for 30 minutes at room temperature in 3% paraformaldehyde/PBS, washed three times with PBS and permeabilized for 30 minutes in 0.5% Triton X-100/5% FCS/2%

BSA/PBS. Cells were subsequently incubated for 1 hour at room temperature with the primary antibodies diluted in the same permeabilization buffer, washed three times in PBS and incubated for 1 hour in the dark with the secondary antibody (Rhodamine- or FITC-conjugated donkey anti-rabbit or anti-mouse IgG, at 1:200 dilution). Coverslips were then washed in PBS and mounted with Gel Mount mounting medium (Biomedica corp. Foster city, CA). Samples were analyzed using a Zeiss laser confocal microscope (Oberkochen, Germany).

For colocalization analyses of internalized FITC-conjugated transferrin, cells were incubated for the last 5 minutes of TPA treatment with 50 μg/ml FITC-conjugated human transferrin. Cells were subsequently processed for immunofluorescence as described above.

Results

Syt II modulates TPA-induced downregulation of PKCα

Consistent with previous results (Huang et al., 1989; Gat-Yablonski and Sagi-Eisenberg, 1990), subjection of RBL cells to a 6 hour treatment with TPA (50 nM) resulted in downregulation of PKCα: ~80% of PKCα was degraded (Fig. 1A). To investigate whether Syt II played a role in this process, we made use of RBL cells in which the level of Syt II expression was suppressed (RBL-Syt II$^-$) by transfection with Syt II antisense cDNA (Baram et al., 1999). Indeed, as shown in Fig. 1, in the RBL-Syt II$^-$ cells, which express less than 5% of normal Syt II levels (Fig. 1A), downregulation of PKCα was considerably inhibited, whereby at the end of the TPA incubation period only 35% of PKCα was degraded (Fig. 1A).

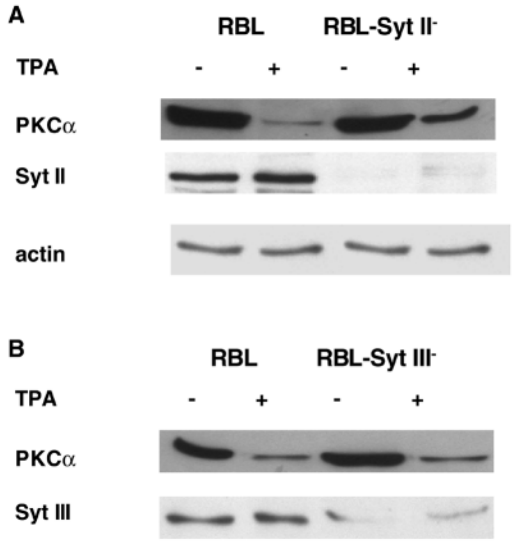

Fig. 1. TPA-induced downregulation of PKCα. Control (empty-vector-transfected) RBL cells (A,B), RBL-Syt II$^-$ cells (A) and RBL-Syt III$^-$ cells (B) were incubated with or without TPA (50 nM) for 6 hours. Whole lysates (40 μg protein) were resolved by SDS-PAGE and immunoblotted. The cellular level of PKCα was determined by western blot analysis using anti PKCα antibodies. The level of Syt II was determined using the monoclonal antibody 8G2B directed against the N-terminus of Syt II. The cellular level of Syt III was determined using a rabbit polyclonal serum directed against the cytoplasmic domain of Syt III. The cellular level of actin was determined to judge for equal loading. Data represent one of three separate experiments.

These results therefore suggested that Syt II may be required for efficient downregulation of PKCα by TPA.

The effect of Syt II was isoform specific, as indicated by the fact that suppression of Syt III, the second most abundant Syt homologue expressed in the RBL cells (Baram et al., 1999), by > 90% (Fig. 1B, lower panel), by transfection with Syt III antisense cDNA (E.G., Z.P., I. Hammel and R.S-E., unpublished) failed to protect PKCα from TPA-induced downregulation. (Fig. 1B).

For the next step, we compared the kinetics of TPA-induced downregulation of PKCα in control cells, RBL-Syt II$^-$ cells and in RBL-Syt II$^+$ cells, in which the level of Syt II expression was increased by two-fold by stable transfection with Syt II sense cDNA (Baram et al., 1999). Notably, we have previously demonstrated that the overexpressed Syt II protein in the RBL-Syt II$^+$ cells was targeted to the same late endosomal/lysosomal compartment that contains the endogenous Syt II protein (Baram et al., 1999). These analyses revealed that reducing or increasing the cellular level of Syt II indeed inhibited or facilitated TPA-induced downregulation, respectively. Hence, whereas the half-life of the kinase in TPA-treated control RBL cells was 2 hours, it was increased to 4 1/4 hours in the RBL-Syt II$^-$ cells and decreased to 1 1/2 hours in the RBL-Syt II$^+$ cells (Fig. 2).

A proteasomal inhibitor prevents TPA-induced downregulation of PKCα

Previous studies have implicated the proteasome in TPA-induced degradation of PKCα (Lu et al., 1998). Thus, proteasome inhibitors prevented the depletion of PKC (Lu et al., 1998). Moreover, a kinase-dead ATP-binding mutant of PKCα could not be depleted by TPA (Lu et al., 1998). Therefore, to identify the proteolytic machinery involved in TPA-induced degradation of PKCα in the RBL cells, we tested the effects of leupeptin, an inhibitor of lysosomal proteases,

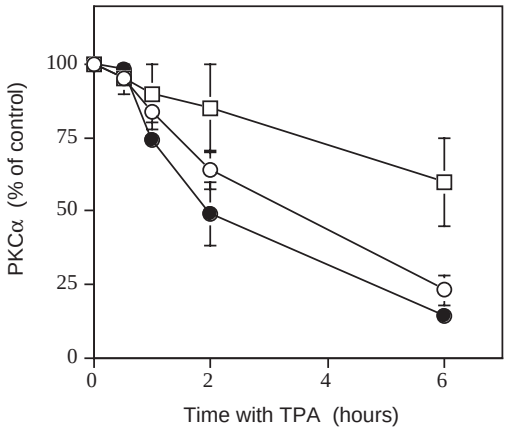

Fig. 2. Kinetics of TPA-induced PKCα degradation. Control empty-vector-transfected RBL cells, RBL-Syt II$^-$ and RBL-Syt II$^+$ cells were treated with TPA (50 nM) for the indicated time periods, and the cellular level of PKCα was determined as described in Fig. 1. The intensities of the bands corresponding to PKCα were quantified by densitometry and are presented as a percentage of the amount of enzyme present in untreated cells. Data represent the average±s.e. of three separate experiments.

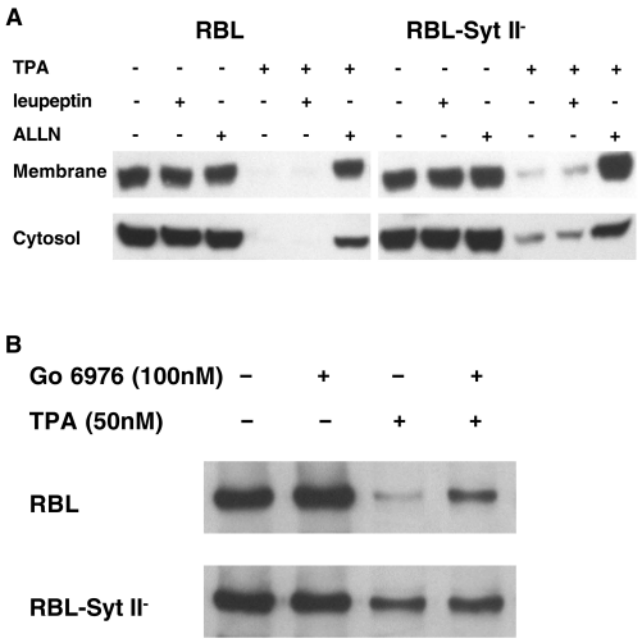

Fig. 3. (A) TPA-induced downregulation of PKCα is sensitive to a proteasome inhibitor. Control (empty-vector-transfected) RBL cells and RBL-Syt II⁻ cells were treated for 12 hours with TPA (50 nM) in the absence or presence of the lysosomal inhibitor (leupeptin, 10 μg/ml) or the proteasomal inhibitor (ALLN, 38.5 μg/ml). Cytosolic and membranal fractions were separated as described in the Materials and Methods, and the amount of PKCα in each fraction was determined as described in Fig. 1. Data represent one of two separate experiments. (B**)** TPA-induced downregulation of PKCα is sensitive to the PKC inhibitor Go 6976. Control (empty vector transfected) RBL cells and RBL-Syt II⁻ cells were treated for 12 hours with TPA (50 nM) in the absence or presence of the PKC inhibitor Go 6976 (100 nM). The cellular level of PKCα was determined as described in Fig. 1. Data represent one of three separate experiments.

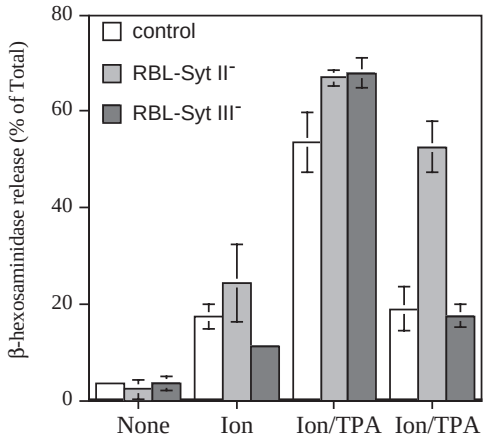

Fig. 4. Modulation of exocytosis. Control (empty-vector-transfected) RBL cells (1-4), RBL-Syt II⁻ cells (5-8) and RBL-Syt III⁻ cells (9-12) were incubated for 30 minutes at 37°C in the presence of buffer (1,5,9), the Ca^{2+} ionophore (A23187, 10 μM, 2,6,10) and the combination Ca^{2+} ionophore (A23187, 10 μM) and TPA (50 nM) without (3,7,11) or with (4,8,12) prior treatment with TPA (50 nM) for 6 hours. The extent of release is presented as a percentage of total cellular β-hexosaminidase activity. Data represent the average±s.e. of three separate experiments.

and ALLN, an inhibitor of the proteasome, on TPA-induced downregulation. In the absence of TPA, neither of these inhibitors affected the levels of PKCα present in the cytosol or the plasma membrane (Fig. 3A). Exposing the cells for 12 hours to TPA resulted in the complete depletion of PKCα from the RBL cells and in the partial depletion of PKCα from the RBL-Syt II⁻ cells (Fig. 3A). In both cell types, pretreatment with leupeptin had no effect (Fig. 3A). Similarly, inhibition of endosomal/lysosomal acidification by chloroquine (50 μM) or NH_4Cl (20 mM) failed to prevent the depletion of PKCα (data not shown). By contrast, inclusion of the proteasome inhibitor ALLN prevented TPA-induced downregulation of PKCα in both the parental RBL cells and in the RBL-Syt II⁻ cells (Fig. 3A).

Depletion of PKCα was prevented when the activity of the enzyme was inhibited by including the PKC inhibitor Go 6976, which specifically blocks the activity of the PKCα and β isoforms (Fig. 3B).

Phorbol-ester-sensitive PKCs remain active in TPA-treated RBL-Syt II⁻ cells

The Ca^{2+} ionophore and TPA interact synergistically to promote exocytosis in RBL cells (Sagi-Eisenberg and Pecht, 1984; Sagi-Eisenberg et al., 1985). Long-term exposure to TPA inhibits this response by downregulating the TPA-responsive PKCs (Gat-Yablonski and Sagi-Eisenberg, 1990). To examine whether protection from degradation also retained PCKα active in the RBL-Syt II⁻ cells, we measured the release of β-hexosaminidase, a marker for exocytosis, in response to triggering with the combination of a Ca^{2+} ionophore (A23187) and TPA before and after prolonged treatment with TPA. In the absence of any stimulus, both RBL and RBL-Syt II⁻ cells spontaneously released less than 5% of their total β-hexosaminidase activity (Fig. 4). Upon exposure to A23187 (10 μM), RBL cells released 17% of their total β-hexosaminidase, whereas RBL-Syt II⁻ cells released 24% (Fig. 4). TPA alone failed to stimulate exocytosis in either the control or the RBL-Syt II⁻ cells (data not shown). However, exposure to A23187 and TPA resulted in the release of 54% and 67% of β-hexosaminidase from the RBL and RBL-Syt II⁻ cells, respectively (Fig. 4). By contrast, in cells pretreated with TPA for 6 hours prior to triggering, subsequent exposure to A23187 and TPA resulted in the release of less than 19% of β-hexosaminidase from RBL cells, whereas the RBL-Syt II⁻ cells retained their responsiveness and released 53% of β-hexosaminidase (Fig. 4). By contrast, 6 hours of treatment of the RBL-Syt III⁻ cells with TPA resulted in the loss of their responsiveness to a subsequent TPA/ionophore trigger (Fig. 4). These results therefore support the notion that suppression of Syt III, unlike that of Syt II, could not repress TPA-induced PKCα downregulation.

The route of PKCα in TPA-treated cells

To investigate the step in PKCα downregulation that was dependent on Syt II, we fractionated TPA-treated cells on linear sucrose gradients to identify the cellular organelles thar

PKCα was associated with. This was carried out in the control RBL cells and the RBL-Syt II⁻ cells and as a function of the TPA incubation period. In resting RBL cells, PKCα was distributed between three major peaks (Fig. 5A). Approximately 65% of the total amount of enzyme were present in fractions 3-10; a smaller amount of the enzyme (~20% of total) was observed at fractions 13-18 and a minor amount (13%) was present at fractions 19-24 (Fig. 5A). On the basis of our previous analyses, fractions 3-10, which run at 0.33-0.70 M sucrose contain the cytosol, as evidenced by lactate dehydrogenase activity (Baram et al., 1999), as well as the early endosomes, as indicated by the migration of several endosomal markers, including the early endosomal antigen 1 (EEA1), annexin II and syntaxin 7. Fractions 13-18, that run at 0.88-1.09 M sucrose, contain the plasma membrane (E.G., Z.P., I. Hammel and R.S-E., unpublished), whereas fractions 19-24 at 1.23-1.45 M sucrose include the SG, on the basis that they contain both histamine and β-hexosaminidase activity (Baram et al., 1999). Thus, in the absence of TPA, most (~65%) of PKCα is localized to the fractions that include cytosol and early endosomes, whereas a smaller amount is distributed between the plasma membrane and the cells SG (Fig. 5C). Following 20 minutes of incubation with TPA, the amount of PKCα present at the light (cytosol/early endosome) fractions decreased to approximately 20% of total, the amount of the plasma-membrane-associated enzyme increased to 40%, and the SG fractions contained 15% of the total cellular amount of enzyme (Fig. 5C). After 2 hours of TPA treatment, the amount associated with the plasma membrane fractions

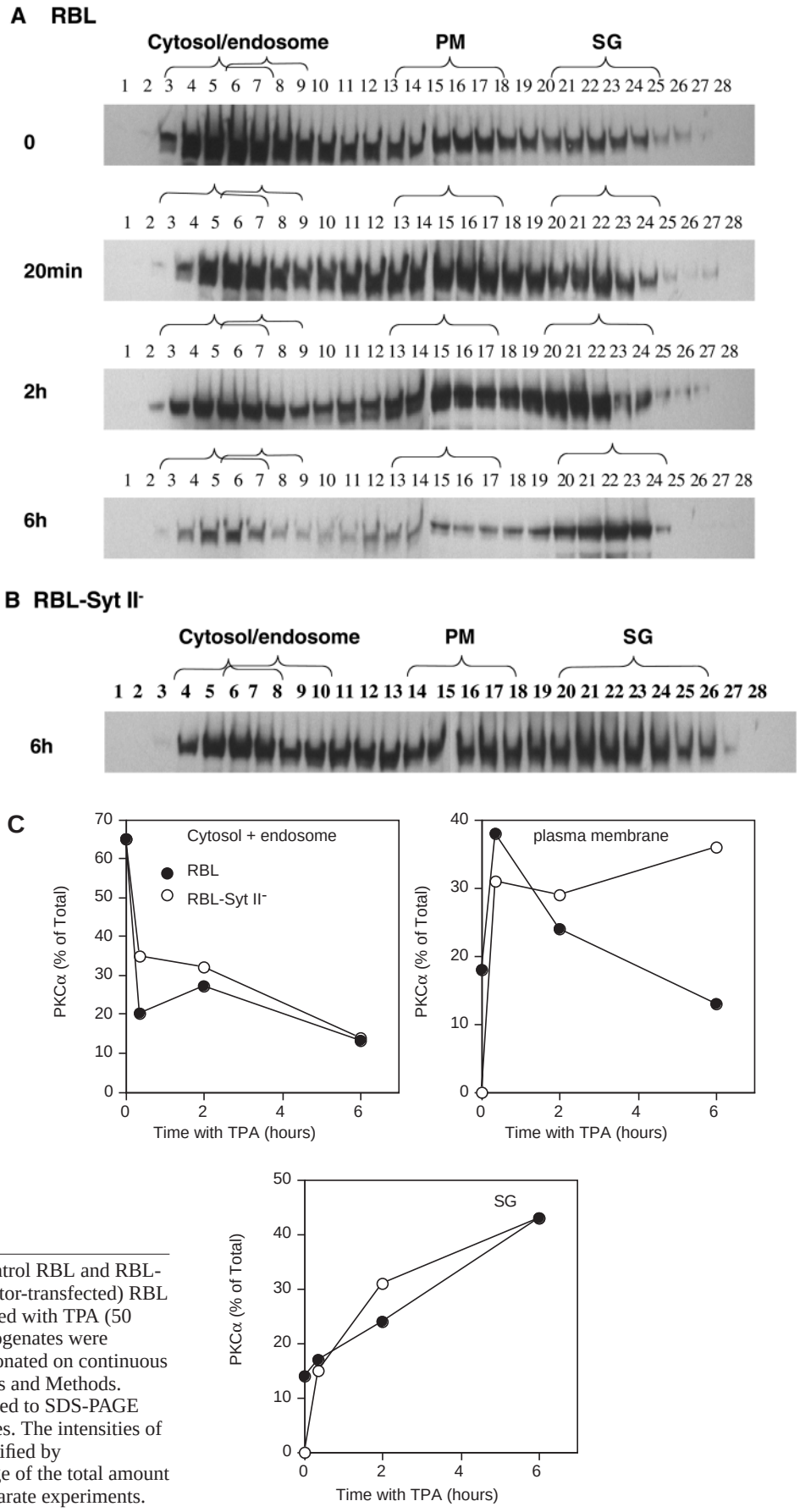

Fig. 5. TPA-stimulated traffic of PKCα in control RBL and RBL-Syt II⁻ cells. Upper panel: control (empty-vector-transfected) RBL cells (A) and RBL-Syt II⁻ (B) cells were treated with TPA (50 nM) for the indicated time periods. Cell homogenates were prepared, and equal amounts of protein fractionated on continuous sucrose gradients as described in the Materials and Methods. Fractions were collected from the top, subjected to SDS-PAGE and immunoblotted with anti-PKCα antibodies. The intensities of the bands corresponding to PKCα were quantified by densitometry and are presented as a percentage of the total amount of enzyme (C). Data represent one of two separate experiments.

decreased with a concomitant increase in the amount of enzyme associated with the SG fractions (Fig. 5). Finally, after 6 hours of TPA incubation, the total amount of PKCα in the cell was markedly reduced and most of the residual enzyme was present at the SG fractions (Fig. 5).

A similar pattern was detected when analyzing fractions derived from non-treated RBL-Syt II– cells or cells subjected to short term (20 minutes or 2 hours) TPA treatment (data not shown). However, two major differences were observed upon increasing the incubation period with TPA to 6 hours. First, the total amount of PKCα present in the cells was considerably higher than that present in the TPA-treated control cells (Fig. 5B). Secondly, in the RBL-Syt II– cells, >30% of the total PKCα was still associated with plasma membrane fractions (Fig. 5B,C). Hence, whereas in both the RBL and RBL-Syt II– cells PKCα was distributed between the cytosol/endosomes, plasma membrane and SG, with increasing exposure time to TPA, the total amount of PKCα in the RBL-Syt II– cells was larger, and a significant fraction of the enzyme remained associated with the plasma membrane fractions.

To substantiate these results further, we also used immunofluorescence and laser confocal microscopy to observe the TPA-induced route of PKCα. Moreover, because our fractionation studies could not distinguish between cytosolic and endosomal fractions, we labeled the latter compartment by allowing the cells to internalize Fluorescein-conjugated transferrin (FITC-Tfn) for 5 minutes. Both non-treated RBL and RBL-Syt II– cells showed a diffuse cytosolic pattern of staining for PKCα (Fig. 6A,A′). TPA treatment for 20 minutes resulted in translocation of the enzyme from the cytosol to the plasma membrane (Fig. 6B,B′). However, in RBL-Syt II– cells, but not in the control RBL cells, PKCα was also present in a perinuclear location (Fig. 6B′). Under these conditions, Tfn localized to peripheral vesicles, which were scattered through the cytosol in the RBL cells (Fig. 6C), whereas in the RBL-Syt II– cells, Tfn was concentrated in a perinuclear structure (Fig. 6C′), where it colocalized with PKCα (Fig. 6D′). After 2 hours of TPA treatment, the amount of PKCα in the RBL cells was markedly reduced, and most of the enzyme showed a granular stain (Fig. 6E). In a few cells the enzyme was also associated with the perinucleus (Fig. 6E). RBL-Syt II– cells contained more PKCα, and the enzyme was still distributed between the plasma membrane and the perinuclear structure (Fig. 6E′). Notably, under these conditions - namely TPA treatment for 2 hours following 5 minutes of internalization - Tfn was targeted to peripheral early endosomes in RBL cells (Fig. 6F) but to the perinuclear location in the RBL-Syt II– cells (Fig. 6F′).

A longer exposure period to TPA (4 hours) almost completely depleted PKCα from the control RBL cells (Fig. 6H), leaving only a minute amount associated with peripheral vesicles. However, these vesicles did not overlap with the Tfn-positive early endosomes (Fig. 6I,J). In contrast, a considerable amount of PKCα was still concentrated in the perinuclear structure in the RBL-Syt II– cells (Fig. 6H′), where it colocalized with internalized Tfn (Fig. 6I′,J′). The remaining enzyme localized to the plasma membrane and to Tfn-negative peripheral vesicles (Fig. 6J′). To investigate whether the perinuclear compartment, which included both Tfn and PKCα, corresponded to the recycling endocytic compartment (recycling endosomes), we stained the cells with an antibody directed against the small GTPase Rab 11, which resides at the recycling compartment (Sheff et al., 1999; Trischler et al., 1999). Indeed, the Tfn-positive compartment present in the TPA-treated RBL-Syt II– cells, overlapped with the Rab 11 staining, confirming its identification as the recycling endosomes (Fig. 7A-C). Because our biochemical fractionation data suggested that PKCα also comigrated with SG containing fractions, we investigated whether the Tfn-negative vesicles with which PKCα was associated corresponded to SG. To this end, we labeled the latter with an antibody directed against the SG

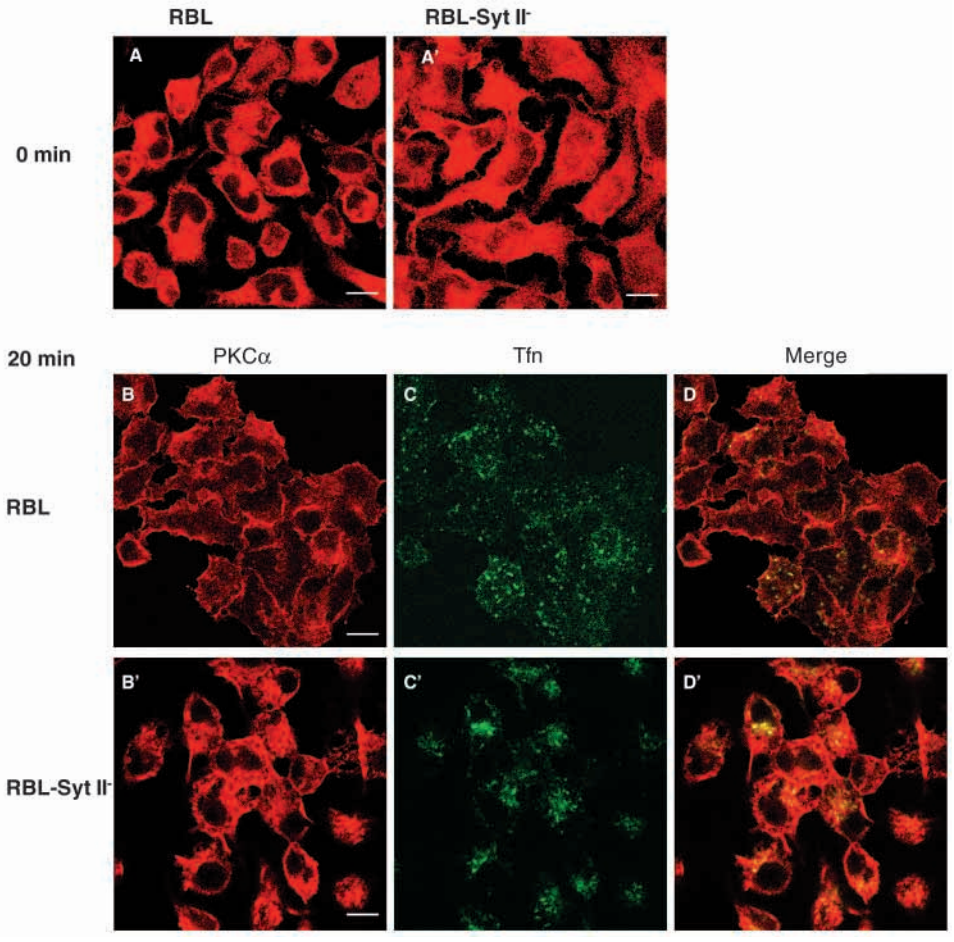

marker serotonin. Indeed, a partial overlap between PKCα and serotonin was clearly demonstrated in both RBL and RBL-Syt II⁻ TPA-treated cells (Fig. 7B,A-F). These results have therefore confirmed that the Tfn-negative peripheral vesicles, with which PKCα was associated in the TPA-treated cells, correspond to the SG.

Discussion

Previous studies have indicated that TPA-induced downregulation of PKCα is traffic dependent (Prevostel et al., 2000). In this work we investigated whether Syt II, a member of the synaptotagmin (Syt) family, influences this downregulation. To this end, we made use of RBL cells, which we stably transfected with sense or antisense Syt II cDNA to overexpress or reduce the level of Syt II expression, respectively. Indeed, we demonstrate that the rate of TPA-induced degradation of PKCα depends on Syt II, whereby overexpression of Syt II reduces the half-life of the enzyme, whereas Syt II suppression increases the half-life two-fold. To monitor the route through which PKCα travels and identify the Syt II-dependent step we employed two experimental approaches, namely fractionation on continuous sucrose gradients and laser confocal microscopy. Taken together, our results indicate that exposure of RBL cells to TPA triggers translocation of the kinase from the cytosol to the plasma membrane, a process that takes 10 to 20 minutes. A 1 to 2 hour exposure then results in the subsequent delivery to early endosomes, where PKCα colocalizes with internalized Tfn. These observations are consistent with previous results demonstrating that PKCα downregulation involves trafficking of the soluble kinase to early endosomes via the plasma membrane and caveolae (Prevostel et al., 2000). A fraction of PKCα is delivered to a perinuclear location, which again is consistent with previous results, where GFP-PKCα, transfected into COS-7 cells was located in a perinuclear compartment (Hansra et al., 1999). We have identified this perinuclear compartment as the perinuclear recycling endosomes on the basis that it contains internalized Tfn and it also stains positive for the recycling endosomal marker, the small GTPase Rab 11 (Sheff et al., 1999; Trischler et al., 1999). Longer exposure to TPA (>4 hours) results in degradation and depletion of the kinase. Notably, consistent with previous results, where a kinase-dead mutant of PKCα could not be depleted (Lu et al., 1998), we show that inhibition of PKCα activity by the specific inhibitor Go 6976 protects PKCα from TPA-induced degradation. Surprisingly, we find a fraction of PKCα associated with the SG of the cells. This conclusion is based upon both biochemical data, demonstrating that PKCα

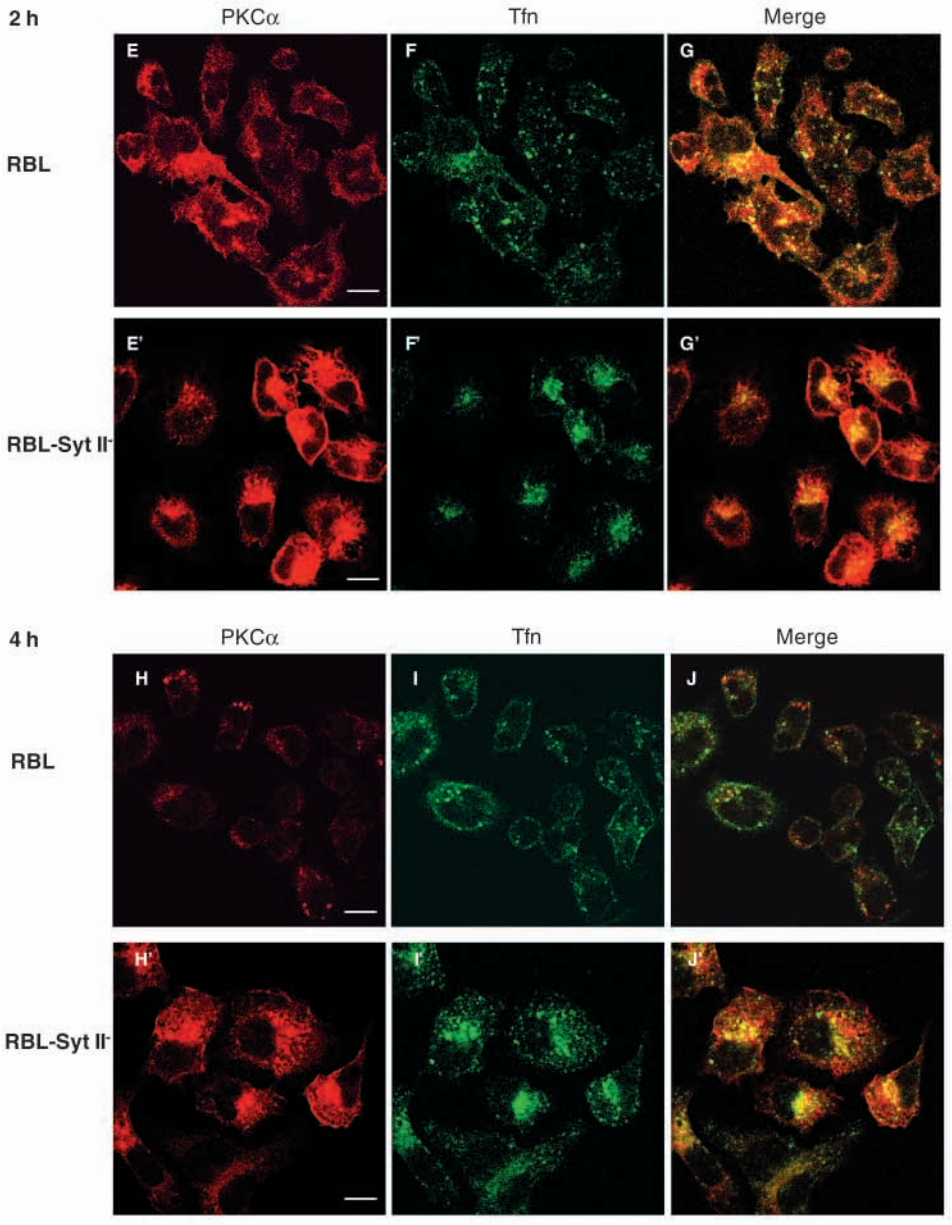

Fig. 6. Immunofluorescence analyses of TPA-dependent traffic of PKCα. Control (empty-vector-transfected) RBL cells (A-J) and RBL-Syt II⁻ cells (A′-J′) were treated with TPA for the indicated time periods: 0 minutes (A,A′); 20 minutes (B-D,B′-D′); 2 hours (E-G,E′-G′); or 4 hours (H-J,H′-J′). During the last 5 minutes of incubation with TPA, FITC-Tfn (50 μg/ml) was added. The cells were subsequently processed for immunofluorescent staining using rabbit polyclonal anti-PKCα antibodies (1:200 dilution) and Rhodamine-conjugated donkey anti-rabbit antibodies. The cells were visualized by confocal microscopy, as described in the Materials and Methods. Red, PKCα; green, Tfn; yellow, overlap. Data represent one of six separate experiments.

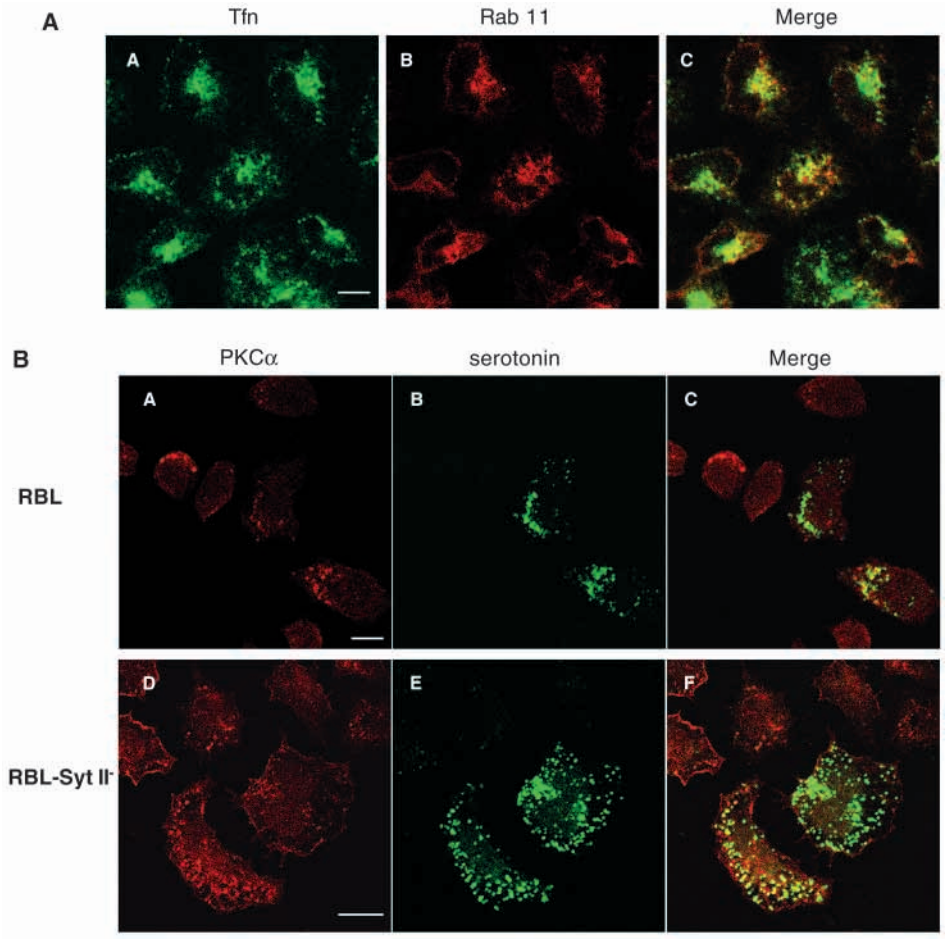

Fig. 7. (A) Tfn-positive endosomes co-stain with Rab 11. RBL-Syt II⁻ cells were treated at 37°C with TPA for 2 hours and incubated with FITC-Tfn (50 μg/ml) for the last 5 minutes of incubation. The cells were subsequently processed for immunofluorescent staining using rabbit polyclonal anti Rab 11 antibodies followed by Rhodamine-conjugated donkey anti-rabbit antibodies. A-Tfn (green), B-Rab 11 (red), C-Merge. Data represent one of two separate experiments. (B) PKCα-positive vesicles co-stain with serotonin. RBL (A-C) and RBL-Syt II⁻ (D-F) cells were treated at 37°C with TPA for 4 hours. The cells were subsequently processed for immunofluorescent staining using rabbit polyclonal anti-PKCα and mouse monoclonal anti-serotonin antibodies followed by Rhodamine-conjugated donkey anti-rabbit antibodies and FITC-conjugated donkey anti-mouse antibodies. A, D-PKCα (red), B, E-serotonin (green), C, F-Merge. Data represent one of three separate experiments.

colocalizes with histamine and serotonin, which are both cargo of mast cell SG, in fractions derived from continuous sucrose gradients (Fig. 5) or by laser confocal immunofluorescence microscopy studies (Fig. 7B), respectively. The physiological implications of this finding are presently unknown. Mast cells undergo exocytosis in a regulated, Ca^{2+}-dependent fashion releasing the contents of their SG and thereby triggering the onset of both immediate and late phase inflammatory reactions. PKCs play a role in stimulus-secretion coupling (Sagi-Eisenberg and Pecht, 1984); however, whether PKCα may also be involved in controlling the exocytic event itself is not known. It should be noted that previous studies have already demonstrated that cargo internalized by RBL cells can reach SG and exocytose in a regulated fashion (Xu et al., 1998), thus indicating an intimate connection between endosomes and the SG.

The major difference in the trafficking of PKCα in RBL versus RBL-Syt II⁻ cells is the amount of enzyme delivered to the perinuclear recycling compartment. Whereas only a small amount of the enzyme seems to reach this compartment in the control cells, a considerably larger amount colocalizes with Tfn in this compartment in the RBL-Syt II⁻ cells. These results

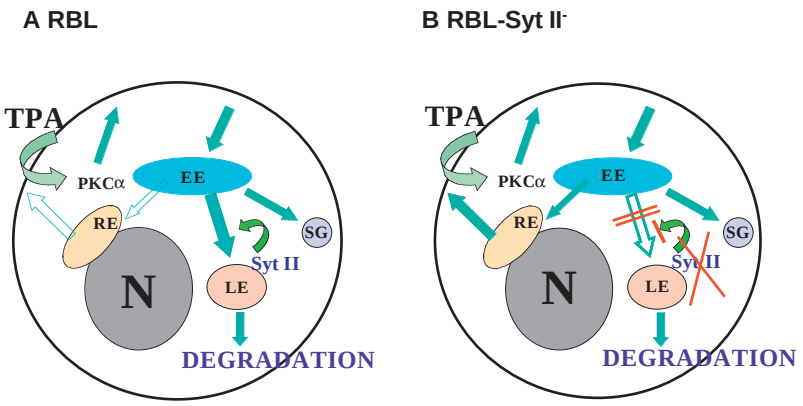

Fig. 8. A model illustrating TPA-induced trafficking of PKCα in RBL cells (A) and RBL-Syt II⁻ cells (B). According to this model, exposure to TPA of the control cells results in translocation of PKCα from the cytosol to the plasma membrane, from where the enzyme is delivered to early endosomes and subsequently a fraction is delivered to the SG, whereas most of the kinase is delivered to late endosomes and degradation. In the RBL-Syt II⁻ cells, the transport to the late endosome and the degradative compartment is retarded because of the reduced amount of Syt II. As a consequence, the kinase is delivered to the recycling endosomal compartment, from where it recycles back to the plasma membrane. EE, early endosomes; RE, recycling endosomes, LE, late endosomes; SG, secretory granules; N, nucleus.

are compatible with a model whereby Syt II is required for the delivery of internalized cargo from early/sorting endosomes to late endosomes and degradation (Fig. 8). Suppression of Syt II thus results in the deviation of endosomal cargo from the degradative pathway to the recycling endosomes. Therefore, while in the control RBL cells active PKCα is delivered from the early/sorting endosomes to degradation, it is targeted to the recycling endosomes in the RBL-Syt II$^-$ cells from where it cycles to the plasma membrane maintaining its active state. Indeed, whereas TPA fails to potentiate Ca^{2+}-ionophore-induced secretion in control cells pretreated for 6 hours with TPA, it still increases by more than two-fold the ionophore-induced secretion in RBL-Syt II$^-$ cells (Fig. 4). Notably, previous studies have implicated PKCs β and ε in mediating secretion triggered by the FcεRI (Ozawa et al., 1993; Chang et al., 1997). Our data suggest that PKCα may be involved in Ca^{2+}-ionophore/TPA-induced secretion, although the possibility that additional isoforms of PKC may also be protected from TPA-induced downregulation in the RBL-Syt II$^-$ cells can not be excluded.

Interestingly, inhibiting the exit from early endosomes towards the late endosomal/lysosomal compartments increases the exit rate towards the recycling endosomes. Thus, whereas in the control cells after 5 minutes of internalization, the majority of Tfn is associated with peripheral vesicles corresponding to the early endosomes, following 5 minutes of internalization by the RBL-Syt II$^-$ cells, most of Tfn already resides in the Rab 11-positive perinuclear recycling compartment. Although the reason for this facilitated delivery to the recycling endosomes is presently unknown, it is possible that Syt II compete with a distinct Syt homologue that is involved in exit from early endosomes towards the recycling compartment for shared effector proteins [SNARE proteins, that constitute the fusion machinery (Adolfsen and Littleton, 2001), or clathrin adaptor proteins (Chapman et al., 1998)]. In the latter case, suppression of Syt II will increase the pool of effectors available for binding to the other Syt homologue and thereby facilitate the exit.

Several observations indicate that the effect of Syt II is isoform specific. First, neither of the other endogenously expressed Syt homologues can substitute for Syt II in the RBL-Syt II$^-$ cells. Second, PKCα is not protected from degradation in RBL-Syt III$^-$ cells in which the expression level of Syt III is reduced by >90%. Finally, the route taken by PKCα in TPA-treated RBL-Syt III$^-$ cells is similar to that of control RBL cells (data not shown). Although not proven here, the ability of Syt II to modulate PKCα downregulation suggests that PKCα is delivered to late endosomes on its route to degradation. Yet neither inhibition of endosomal acidification by chloroquine (50 μM) or NH_4Cl (20 mM) nor exposure to the lysosomal inhibitor leupeptin prevent this degradation. By contrast, degradation is prevented by the proteasome inhibitor ALLN. What the relationship is between the proteasome and the endocytic compartments and how PKCα is delivered from the endosome to the proteasome is presently unknown. Recent studies have demonstrated a mutual requirement for the proteasome and late endosomes/lysosomes in the downregulation of membrane receptors such as MET (Hammond et al., 2001), the GH receptor (Van Kerhof and Strous, 2001) and the receptor for interleukin 2β (Rocca et al., 2001). This may thus also be the case for PKCα downregulation.

In conclusion, our studies indicate that Syt II plays a an active regulatory and physiological role in membrane trafficking. Moreover, by targeting signaling molecules to lysosomes, Syt II may serve as an important regulator of cell signaling, whose level of expression and proper function may define the duration of a signal by controlling receptor as well as effector downregulation.

We thank L. Mitelman for his help in all the microscopy studies. We thank Y. Zick and D. Neumann for helpful discussions and critical reading of this manuscript, T. C. Sudhof, S. Seino, M. Takahashi, Y. Shoji-Kasai and M. Zerial for their generous gifts of cDNAs and antibodies. This work was supported by grants from the Israel Science Foundation, founded by the Israel Academy for Sciences and Humanities and by the Israel Ministry of Health (R.S.-E.).

References

Adolfsen, B. and Littleton, J. T. (2001). Genetic and molecular analysis of the synaptotagmin family. *Cell. Mol. Life Sci.* **58**, 393-402.

Armstrong, J. (2000). How do Rab proteins function in membrane traffic? *Int. J. Biochem. Cell Biol.* **32**, 303-307.

Baram, D., Adachi, R., Medalia, O., Tuvim, M., Dickey, B., Mekori, Y. A. and Sagi-Eisenberg, R. (1999). Synaptotagmin II negatively regulates Ca^{2+}-triggered exocytosis of lysosomes in mast cells. *J. Exp. Med.* **189**, 1649-1658.

Baram, D., Mekori, Y. A. and Sagi-Eisenberg, R. (2001). Synaptotagmin regulates mast cell functions. *Immunol. Rev.* **179**, 25-34.

Bennett, M. K. (1995). SNAREs and the specificity of transport vesicle targeting. *Curr. Opin. Cell Biol.* **7**, 581-586.

Brose, N., Petrenko, A. G., Sudhof, T. C. and Jahn, R. (1992). Synaptotagmin: a calcium sensor on the synaptic vesicle surface. *Science* **256**, 1021-1025.

Chang, E. Y., Szallasi, Z., Acs, P., Raizada, V., Wolfe, P. C., Fewtrell, C., Blumberg, P. M. and Rivera, J. (1997). Functional effects of overexpression of protein kinase C-alpha, -beta, -delta, -epsilon, and -eta in the mast cell line RBL-2H3. *J. Immunol.* **159**, 2624-2632.

Chapman, E. R., Desai, R. C., Davis, A. F. and Tornehl, C. K. (1998). Delineation of the oligomerization, AP-2 binding, and synprint binding region of the C2B domain of synaptotagmin. *J. Biol. Chem.* **273**, 32966-32972.

Gat-Yablonski, G. and Sagi-Eisenberg, R. (1990). Differential down regulation of protein kinase C selectively effects IgE-dependent exocytosis and inositol trisphosphate formation. *Biochem. J.* **270**, 679-684.

Geppert, M., Goda, Y., Hammer, R. E., Li, C., Rosahl, T. W., Stevens, C. F. and Sudhof, T. C. (1994). Synaptotagmin I: a major Ca^{2+} sensor for transmitter release at a central synapse. *Cell* **79**, 717-727.

Hammond, D. E., Urbe, S., Vande Woude, G. F. and Clague, M. J. (2001). Down-regulation of MET, the receptor for hepatocyte growth factor. *Oncogene* **20**, 2761-2770.

Hansra, G. Garcia-Paramio, P., Prevostel, C., Whelan, R. D., Bornancin, F. and Parker, P. J. (1999). Multisite dephosphorylation and desensitization of conventional protein kinase C isotypes. *Biochem. J.* **342**, 337-344.

Huang, F. L., Yoshida, Y., Cunha-Melo, J. R., Beaven, M. A. and Huang, K. P. (1989). Differential down regulation of protein kinase C isozymes. *J. Biol. Chem.* **264**, 4238-4243.

Lowe, M. (2000). Membrane transport: tethers and TRAPPs. *Curr. Biol.* **10**, R407-R409.

Lu, Z., Liu, D., Hornia, A., Devonish, W., Pagano, M. and Foster, D. A. (1998). Activation of protein kinase C triggers its ubiquitination and degradation. *Mol. Cell. Biol.* **18**, 839-845.

McNew, J. A., Weber, T., Parlati, F., Johnston, R. J., Melia, T. J., Sollner, T. H. and Rothman, J. E. (2000). Close is not enough: SNARE-dependent membrane fusion requires an active mechanism that transduces force to membrane anchors. *J. Cell Biol.* **150**, 105-117.

Mellor, H. and Parker, P. J. (1998). The extended protein kinase C superfamily. *Biochem. J.* **332**, 281-292.

Mineo, C., Ying, Y. S., Chapline, C., Jaken, S. and Anderson, R. G. (1998). Targeting of protein kinase C alpha to caveolae. *J. Cell Biol.* **141**, 601-610.

Nishizuka, Y. (1986). Studies and perspectives of protein kinase C. *Science* **233**, 305-312.

Ozawa, K., Yamada, K., Kazanietz, M. G., Blumberg, P. M. and Beaven, M. A. (1993). Different isozymes of protein kinase C mediate feedback inhibition of phospholipase C and stimulatory signals for exocytosis in rat RBL-2H3 cells. *J. Biol. Chem.* **268**, 2280-2283.

Pelech, S. L., Meier, K. E. and Krebs, E. G. (1986). Rapid microassay for protein kinase C translocation in Swiss 3T3 cells. *Biochemistry* **25**, 8348-8353.

Prevostel, C., Alice, V., Joubert, D. and Parker, P. J. (2000). Protein kinase C (alpha) actively down-regulates through caveolae-dependent traffic to an endosomal compartment. *J. Cell Sci.* **113**, 2575-2584.

Razin, E., Zhang, Z. C., Nechushtan, H., Frenkel, S., Lee, Y. N., Arudchandran, R. and Rivera, J. (1999). Suppression of microphthalmia transcriptional activity by its association with protein kinase C-interacting protein 1 in mast cells. *J. Biol. Chem.* **274**, 34272-34276.

Rocca, A., Lamaze, C., Subtil, A. and Dautry-Varsat, A. (2001). Involvement of the ubiquitin/proteasome system in sorting of the interleukin 2 receptor beta chain to late endocytic compartments. *Mol. Biol. Cell* **12**, 1293-1301.

Sagi-Eisenberg, R. and Pecht, I. (1984). Protein kinase C, a coupling element between stimulus and secretion of basophils. *Immunol. Lett.* **8**, 237-241.

Sagi-Eisenberg, R., Lieman, H. and Pecht, I. (1985). Protein kinase C regulation of the receptor-coupled calcium signal in histamine-secreting rat basophilic leukemia cells. *Nature* **313**, 59-60.

Sheff, D. R., Daro, E. A., Hull, M. and Mellman, I. (1999). The receptor recycling pathway contains two distinct populations of early endosomes with different sorting functions. *J. Cell Biol.* **145**, 123-139.

Sudhof, T. C. and Rizo, J. (1996). Synaptotagmins: C2-domain proteins that regulate membrane traffic. *Neuron* **17**, 379-388.

Trischler, M., Stoorvogel, W. and Ullrich, O. (1999). Biochemical analysis of distinct Rab5- and Rab11-positive endosomes along the transferrin pathway. *J. Cell Sci.* **112**, 4773-4783.

Van Kerkhof, P. and Strous, G. J. (2001). The ubiquitin-proteasome pathway regulates lysosomal degradation of the growth hormone receptor and its ligand. *Biochem. Soc. Trans.* **29**, 488-493.

Xu, K., Williams, R. M., Holowka, D. and Baird, B. (1998). Stimulated release of fluorescently labeled IgE fragments that efficiently accumulate in secretory granules after endocytosis in RBL-2H3 mast cells. *J. Cell Sci.* **111**, 2385-2396.